

## Article

# An Intelligent Design Method for Remanufacturing Considering Remanufacturability and Carbon Emissions

Peng Peng <sup>1</sup>, Chao Ke <sup>2,\*</sup> and Jun Han <sup>2</sup>

<sup>1</sup> School of Design, Jiangnan University, Wuxi 214122, China; pengpeng791226@gmail.com

<sup>2</sup> School of Art & Design, Wuhan Institute of Technology, Wuhan 430070, China; 08121204@wit.edu.cn

\* Correspondence: 22121401@wit.edu.cn

**Abstract:** Design for remanufacturing (DfRem) is to consider the remanufacturability of the product at the design stage, which can improve the remanufacturability of the product. Moreover, the DfRem solution has a significant impact on the carbon emissions of manufacturing processes. Unreasonable design solutions can significantly increase carbon emissions from manufacturing processes. However, there is no direct link between DfRem solutions and remanufacturability as well as manufacturing carbon emissions, which makes it difficult to quickly generate a rational DfRem solution that can enhance product remanufacturability and reduce carbon emissions simultaneously. To this end, this paper proposes an intelligent design method for remanufacturing that considers remanufacturability and manufacturing carbon emissions. First, an intelligent DfRem framework is constructed, which includes information acquisition, virtual model construction of the DfRem solution, and multi-objective optimization of the design solution. Then, the design matrix and sensitivity analysis are used to construct the mapping models between remanufacturability, carbon emissions, and DfRem parameters. Meanwhile, a multi-objective optimization model of DfRem with remanufacturability requirements and carbon emissions as design objectives is constructed, and an adaptive teaching and learning optimization algorithm is applied to solve the optimization model to obtain a DfRem solution that satisfies the objective information. Finally, the feasibility of the method is verified by DfRem of the injection mold as an example.



**Citation:** Peng, P.; Ke, C.; Han, J. An Intelligent Design Method for Remanufacturing Considering Remanufacturability and Carbon Emissions. *Processes* **2023**, *11*, 3359. <https://doi.org/10.3390/pr11123359>

Academic Editor: Raul D. S. G. Campilho

Received: 18 October 2023

Revised: 29 November 2023

Accepted: 1 December 2023

Published: 3 December 2023



**Copyright:** © 2023 by the authors. Licensee MDPI, Basel, Switzerland. This article is an open access article distributed under the terms and conditions of the Creative Commons Attribution (CC BY) license (<https://creativecommons.org/licenses/by/4.0/>).

## 1. Introduction

Remanufacturing is the process of turning used blanks into remanufactured products that meet functional and performance requirements through a series of repair techniques. While remanufacturing is the repair and upgrading of valuable parts and components of used products, the maximization of the residual value of used products, and remanufacturing promotes the recycling of used resources, which is increasingly recognized as an important part of the circular economy [1,2]. Remanufacturability determines the successful implementation of used products for remanufacturing. Design for remanufacturing is to consider the remanufacturability of products at the product design stage, which directly affects the product remanufacturability and carbon emissions from the manufacturing process [3,4]. Thus, design for remanufacturing is a key aspect of remanufacturing engineering.

However, remanufacturability, carbon emission, and design parameters are not directly related, making it difficult to quickly generate a DfRem solution that meets the design objectives. To address these issues, many scholars have studied DfRem. Gong et al. [5] proposed a nonempirical hybrid multi-attribute decision-making method, which can alleviate the impacts of subjective factors. Ke et al. [6] developed an intelligent design method for remanufacturing, which can intelligently analyze remanufacturability requirements and

generate design solutions. Zhang et al. [7] analyzed the product engineering characteristics and remanufacturing design guidelines, used the two-stage quality function development method to analyze the impact of failure modes on remanufacturing design, and found an improvement direction for remanufacturing design. Yang et al. [8] proposed a multi-criteria decision method to select the optimal material to improve the remanufacturability of products from the perspective of material selection. Kishawy et al. [9] defined the concepts and needs related to the sustainability approach. Soh et al. [10] provided a holistic approach to designing products from the remanufacturing perspective, considering the disassembly guidelines and constraints. Shahbazi et al. [11] investigated how circular product design can facilitate automation remanufacturing processes. Chakraborty et al. [12] identified the design criteria of a product that can enhance its remanufacturability and subsequently. The above-mentioned literature shows that many scholars conduct research on DfRem methods from the perspectives of failure characteristics, knowledge reuse, material selection, and DfRem scheme evaluation. Undoubtedly, the proposed methods greatly contributed to the research of DfRem. However, these studies have not constructed a relationship between design parameters and remanufacturability, which does not ensure that the design solution precisely satisfies product remanufacturability requirements. In addition, these studies do not take into account the impact of DfRem on manufacturing carbon emissions to ensure that the product manufacturing process is decarbonized. In the axiomatic design (AD) theory, product design parameters directly affect manufacturing process parameters, and process parameters directly affect product manufacturing carbon emissions; therefore, DfRem directly affects the magnitude of manufacturing carbon emissions. In summary, DfRem not only affects the product remanufacturability but also directly affects the manufacturing carbon emissions; excessive carbon emissions will take away the advantages of DfRem.

For developing a reasonable DfRem scheme to reduce carbon emissions, it is necessary to construct the mapping relationship between design parameters and carbon emissions, and many studies have been conducted on this; for instance, low-carbon design considering human behavior [13], product design on remanufacturing considering environment legislation [14], low-carbon design of product family [15], and CAD-based identification of product low-carbon design [16]. This research has analyzed the impact of product design on carbon emissions. Yet, these methods do not simultaneously consider the impact of design parameters on remanufacturability, which does not provide a reasonable DfRem scheme. For the synergistic optimization of these two, it is necessary to build a mathematical model between design parameters, remanufacturability, and carbon emissions.

Previous researchers have made some achievements in relationship construction. Existing research has focused on low-carbon design [17], cost-constraint low-carbon product design [18], and performance-based product design [19]. These studies construct links between cost, performance, carbon emissions, and product design, which reduce product manufacturing costs and carbon emissions and improve product performance. Yet, none of them synergistically consider the impact and mapping of product design on remanufacturability and carbon emissions. The remanufacturability represents the function or product performance, such as easily disassembled, easily recycled, easily processed, etc., and the mathematical relationship between the design parameters and the function can be described by the design matrix in the axiomatic design (AD) theory [20], while sensitivity analysis can analyze the degree of influence between variables and determine the degree of correlation between them [21]; thus, these methods can be used to construct mathematical models between design parameters and remanufacturability and carbon emissions.

Moreover, DfRem is a multi-objective optimization problem, and it is necessary to ensure that remanufacturability and carbon emissions are synergistically satisfied. Many scholars currently use optimization algorithms to optimize design solutions, and multi-objective optimization model-solving algorithms have been developed and are very mature. Commonly used examples include particle swarm algorithms [22], genetic algorithms [23], ant colony algorithms [24], etc., but these algorithms do not have enough computational

accuracy, and their stability is poor. In order to solve the limitations of previous algorithms, an adaptive teaching–learning-based optimization (ATLBO) algorithm is proposed, which simulates the process of students learning from teachers and can adaptively adjust the learning method to achieve faster learning results after learning certain knowledge [25]. The algorithm can avoid entering the local optimum too early, improve the global search ability, speed up the solution, and respond to changes in the optimization model faster.

For the rapid generation of a sound DfRem scheme, it is necessary to construct a mapping model between carbon emissions, remanufacturability, and design parameters and generate a design scheme with an intelligent approach. To address these, an intelligent design method for remanufacturing considering remanufacturability and carbon emission is proposed. The novelty of this study lies in the following: (1) An intelligent design framework is built, which includes design mapping model construction, optimal design solution solving, and a design solution feedback adjustment mechanism. (2) A design matrix and sensitivity analysis are used to construct the mapping models between remanufacturability, carbon emissions, and design parameters. (3) A multi-objective optimization model of the DfRem scheme is constructed, and an improved teaching and learning algorithm is applied to solve the optimization scheme, which realizes the intelligence of DfRem. The effectiveness and feasibility of this method are verified by a case to provide theoretical support for DfRem.

## 2. Methods

### 2.1. Intelligent Design Framework for Remanufacturing

The ultimate goal of DfRem is to realize the functionality and remanufacturability requirements of the customer, while the design process also needs to consider the designer's preferences, manufacturing scenario constraints, policy limitations, etc. Therefore, the DfRem solution needs to be optimized according to the external conditions and constraints so as to make the original design solution conform to the actual application scenarios. Firstly, feedback from customers, designers, and technicians is collected, including remanufacturability requirements, low-carbon requirements, environmental requirements, etc. At the same time, virtual simulation technology is used to construct a virtual product model that meets the design scheme and establish an optimization model for the product design scheme. Finally, the ATLBO algorithm is used to solve the optimization model, and the virtual model is changed according to the optimization results to verify its feasibility. Through the continuous cycle of optimization and feedback, the optimal product design scheme is obtained, and the specific process model is as follows.

As shown in Figure 1, the physical side refers to all the physical entities involved in the product design, including the customers, designers, process engineers, operators, etc. The information side represents all the information generated by the physical entity, i.e., demand information, subjective intent, and environmental demand information, etc. The model side is mainly to build the design optimization model and virtual simulation model. The physical data side represents the historical data of the entire product lifecycle. Moreover, the empty rectangles indicate that there are other categories of people, information, data, etc. For example, the physical side also contains operators and remanufacturers. The adaptive optimization process for DfRem solutions is divided into three main parts:

#### (1) Information acquisition.

The external constraint information of product design includes customer demand information, the designer's personal preference information, the technician's process planning information, environmental laws and regulations, etc. This information provides the constraints and design goals for the implementation of the design program. The above information is mainly summarized into four aspects: performance requirements, cost requirements, energy saving, and emission reduction. The internal connection between the target information and the design parameters is analyzed, and the mapping mathematical model is constructed between the two so as to facilitate the optimization of the subsequent design parameters.

(2) Construction of the design scheme virtual model.

In order to realize the visualization of the design scheme, the virtual model of the design scheme is constructed, including the physical model of the new product, the performance simulation model, the cost analysis model, the energy saving and emission reduction analysis model, and the processing simulation model, etc. The virtual model can quickly verify the feasibility of the design scheme, reduce the trial-and-error cost, and shorten the design cycle.

(3) Multi-objective optimization of DfRem solutions.

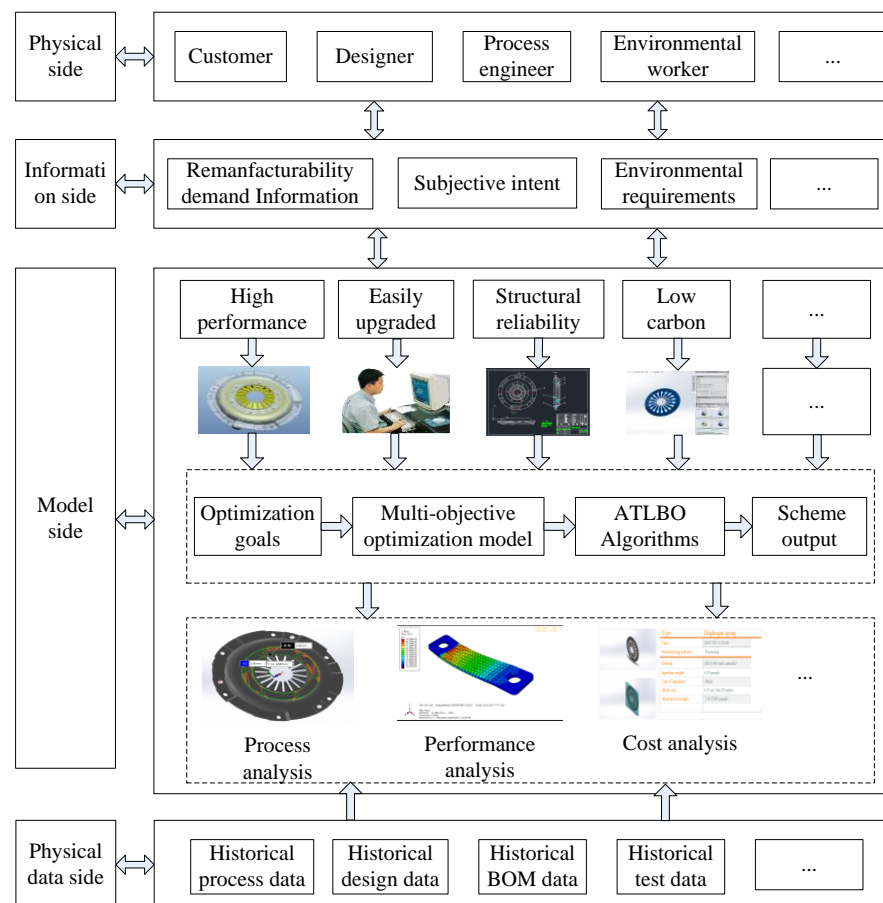


**Figure 1.** Intelligent design framework for remanufacturing.

The design scheme multi-objective optimization model with manufacturing costs, remanufacturing performance requirements, and carbon emissions as design objectives is constructed, and the optimization model is solved by using adaptive teaching and learning optimization algorithms to obtain the design scheme that satisfies the objective information.

## 2.2. Information Extraction and Optimization Objective Analysis

Once the DfRem scheme is completed, it will be fed back to the customer, process personnel, and safety and environmental departments for program evaluation, and the designers will also verify the performance, structure, and other parameters of the design scheme and put forward new design intentions. The above information will form new design constraints, and at this time, the design solution needs to be based on the constraints of the information to make changes to the design parameters. The feedback information of the DfRem scheme is categorized from three perspectives of technology, economy, and environment, mainly including remanufacturing performance requirement information, manufacturing cost information, and carbon emission information, as follows:

(1) Information on remanufacturing performance requirements.

After the product design scheme is generated, the development department will carry out prototype trial production and verification according to the scheme. Among them, the performance of parts and the whole machine is tested according to standard operating conditions to ensure that the product can be easily remanufactured after retirement. During the testing process, parts performance that is not up to standard or non-ideal running states will appear; at this time, there is a need to improve the product structure parameters or material parameters to adjust the performance parameters of the product. Product performance information is mainly collected through testing equipment, sensors, and collection devices, according to the collected performance data and customer performance requirements and remanufacturing performance standards for comparison to extract the performance parameters that need to be improved.

(2) Manufacturing costs.

Manufacturing costs are the core concern of manufacturers, and customers often set the control range of product development costs, so manufacturers must rationalize the manufacturing costs in the production process. Manufacturing costs are mainly material costs, equipment development costs, labor hour costs, commissioning costs, and surcharges. In the actual processing process, there may be more than the predetermined costs, so it is necessary to rationalize the design parameters to reduce the manufacturing costs.

(3) Low-carbon requirements.

The manufacturing process consumes energy such as electricity, water, and oil and generates a large amount of pollutants, including wastewater, metal waste, and waste oil. According to the policies and regulations of energy conservation and emission reduction, as well as the dual-carbon goal, it is necessary to vigorously reduce the consumption and emission of these two parts. In order to characterize the energy conservation and emission reduction goal, carbon emission can be used to represent the energy consumption in the manufacturing process and the energy consumption of waste treatment.

The constraint information is extracted to analyze the optimization objective of the design scheme, and the establishment of the connection between the constraint information and the design parameters is the key to the optimization of the design scheme; below is the model developed by the authors.

#### 2.2.1. Mapping Model of Remanufacturability and DfRem Parameters

The remanufacturability demand includes easy to disassemble, easy to clean, easy to reprocess, etc., which correspond to the stiffness of the product, the strength of the component, the hardness, etc.; the details are shown in Figure 2.

While the mapping relationship between remanufacturability and DfRem parameters can be derived from empirical formulas or theorems, the generic functional relationship between the two can be characterized by using the design matrix in axiomatic design as follows.

$$\begin{Bmatrix} F_1 \\ F_2 \\ \dots \\ F_m \end{Bmatrix} = \begin{bmatrix} A_{11} & A_{12} & \dots & A_{1j} & \dots & A_{1n} \\ A_{21} & A_{22} & \dots & A_{2j} & \dots & A_{2n} \\ \dots & \dots & \dots & \dots & \dots & \dots \\ A_{i1} & A_{i2} & \dots & A_{ij} & \dots & A_{in} \\ \dots & \dots & \dots & \dots & \dots & \dots \\ A_{m1} & A_{m2} & \dots & A_{mj} & \dots & A_{mn} \end{bmatrix} \begin{Bmatrix} DP_1 \\ DP_2 \\ \dots \\ DP_n \end{Bmatrix} \quad (1)$$

Therefore, the remanufacturability requires multiple DfRem parameters to be solved, which can be shown by Equation (2):

$$F_i = \sum_{j=1}^n A_{ij} \cdot DP_j \quad (2)$$

where  $F_m$  denotes the  $m$ -th remanufacturability of the product,  $DP_n$  denotes the  $n$ -th DfRem parameter, and  $A_{ij}$  denotes the mapping relationship between the  $i$ -th remanufacturability and the  $j$ -th DfRem parameter, which can be either a real number or a functional relationship.

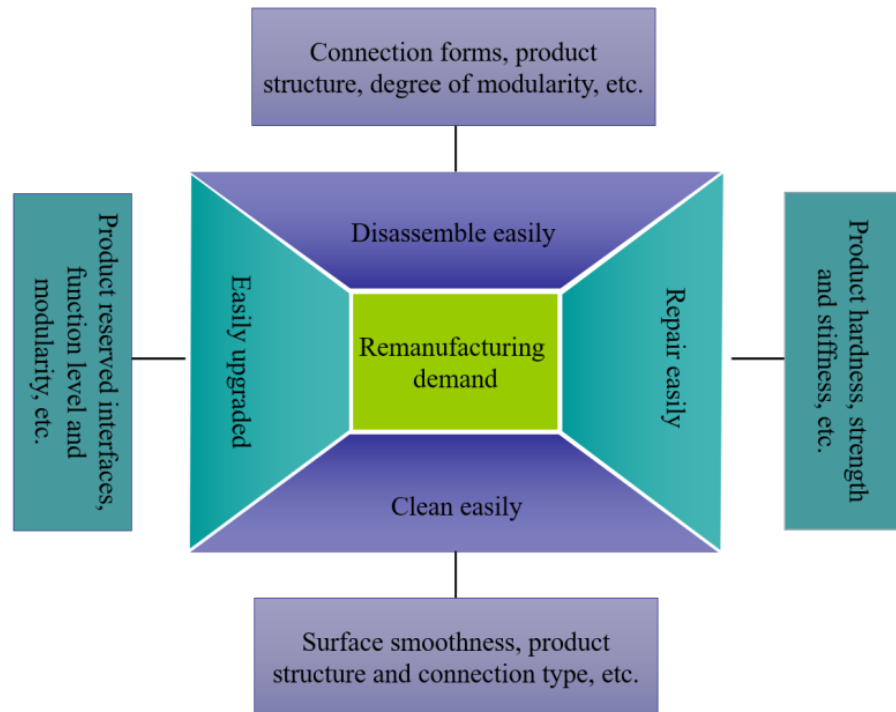


**Figure 2.** The categories of remanufacturability demand.

#### 2.2.2. Mapping Relationship between Carbon Emissions and Design Parameters

Carbon emissions from product manufacturing are directly related to the DfRem parameter. Carbon emissions are mainly generated by consumed electricity, water, raw materials, weather, etc. Firstly, a carbon emission calculation model should be established, and then a mapping relationship between energy consumption, material consumption, and design parameters should be established using sensitivity analysis; below is the model developed by the authors.

Different energy and materials are consumed in the manufacturing process of the product, and these generate carbon emissions, so the consumption of energy and materials can be counted to calculate the manufacturing carbon emissions.

$$H_i = \sum_{q=1}^p N_q^E f_q^E + \sum_{t=1}^n N_t^M f_t^M \quad (3)$$

In Equation (3),  $H_i$  denotes the manufacturing carbon emission corresponding to the  $i$ -th DfRem parameter,  $N_q^E$  denotes the  $q$ -th energy consumption,  $f_q^E$  denotes the carbon emission factor of the  $q$ -th energy source,  $N_t^M$  represents the  $t$ -th material consumption, and  $f_t^M$  denotes the carbon emission factor of the  $t$ -th material.

In order to obtain the functional relationship between carbon emissions and design parameters, it can be analyzed by sensitivity, which can be obtained by the relationship between the number of micro-variations between carbon emissions and design parameters; below is the model developed by the authors.

$$S_i = \frac{dH_i}{dDP_i} = \frac{df_{H_i}(DP_i)}{dDP_i} \quad (4)$$

Equation (4) represents manufacturing carbon emissions as a function of trace changes in design parameters,  $f_{H_i}$  represents the function between energy consumption and the design parameters, and  $S_i$  denotes the sensitivity coefficient of the  $i$ -th design parameter to the corresponding carbon emission.

By converting Equation (4), the mapping relationship between the micro variables of carbon emissions and the micro variables of DfRem parameters can be obtained, and the details are shown in Equation (5).

$$dH_i = S_i \cdot dDP_i \quad (5)$$

The functional relationship between carbon emissions and DfRem parameters can be obtained by solving the differential equation, which is shown as follows.

$$H_i = S_i \cdot DP_i + g_i \quad (6)$$

The result of solving Equation (3) is shown in Equation (6), where  $g_i$  represents the constant of the  $i$ -th carbon emission equation.

### 2.2.3. Manufacturing Cost Constraint

Process engineers formulate the corresponding process program according to the design and processing by the manufacturing shop. The design scheme directly determines the manufacturing process of the parts but also determines the processing of electricity, water, materials, and other energy consumption; an increase in consumption will undoubtedly increase the cost of manufacturing products. Each processing scheme will contain different processing methods to achieve, and each processing method will use the appropriate processing equipment, raw materials, and heat treatment; processing will also consume different amounts of energy, so it is necessary to analyze according to the specific object. In this paper, the cost of manufacturing is the constraint of the design scheme.

### 2.3. Optimization Model Construction

In order to improve design efficiency, product remanufacturability, and reduce carbon emissions, the optimization model of the DfRem scheme is built with remanufacturability and carbon emission, and an intelligent algorithm is applied to solve the DfRem scheme. Meanwhile, virtual verification of the product remanufacturability and manufacturing process is carried out by using physical modeling, CAE simulation, and energy consumption evaluation technologies, and the verification results are fed back to the subject demand departments, which compare and analyze according to historical physical data, and feed the analysis results to the optimization process as design objectives until the optimal design results are obtained. The detailed process is shown in Figure 3.

The optimization model is constructed with the objectives of remanufacturability and manufacturing carbon emissions. According to the axiomatic design matrix, the performance is equal to the product of the mapping parameter and the design parameter, while the product of the two is inverted for the minimum optimization principle, which is shown in Equation (7). The carbon emission minimization optimization objective function is shown in Equation (8).

$$\min F_i = \frac{1}{A_{ij} * DP_j} \quad (7)$$

$$\min H = \sum_{i=1}^n (S_i \cdot DP_i + g_i) \quad (8)$$

The constraints of the optimization model are set according to the system requirements, manufacturing cost requirements, and legal policies. The details are as follows:

$$C_s < C < C_d \quad (9)$$

$$H < H_l \quad (10)$$

$$DP_{lp} \leq DP_i \leq DP_{up} \quad (11)$$

where  $C_s$  denotes the manufacturer's constraint value for manufacturing cost, and  $C_d$  denotes the customer's constraint value for product manufacturing cost; in general, the manufacturing cost set by the manufacturer will be lower than the manufacturing cost set by the customer.  $H_l$  denotes the carbon emission limit set by policy and regulation. The lower and upper limits of the DfRem parameters are determined by the product system constraints, tolerance range, and other factors.

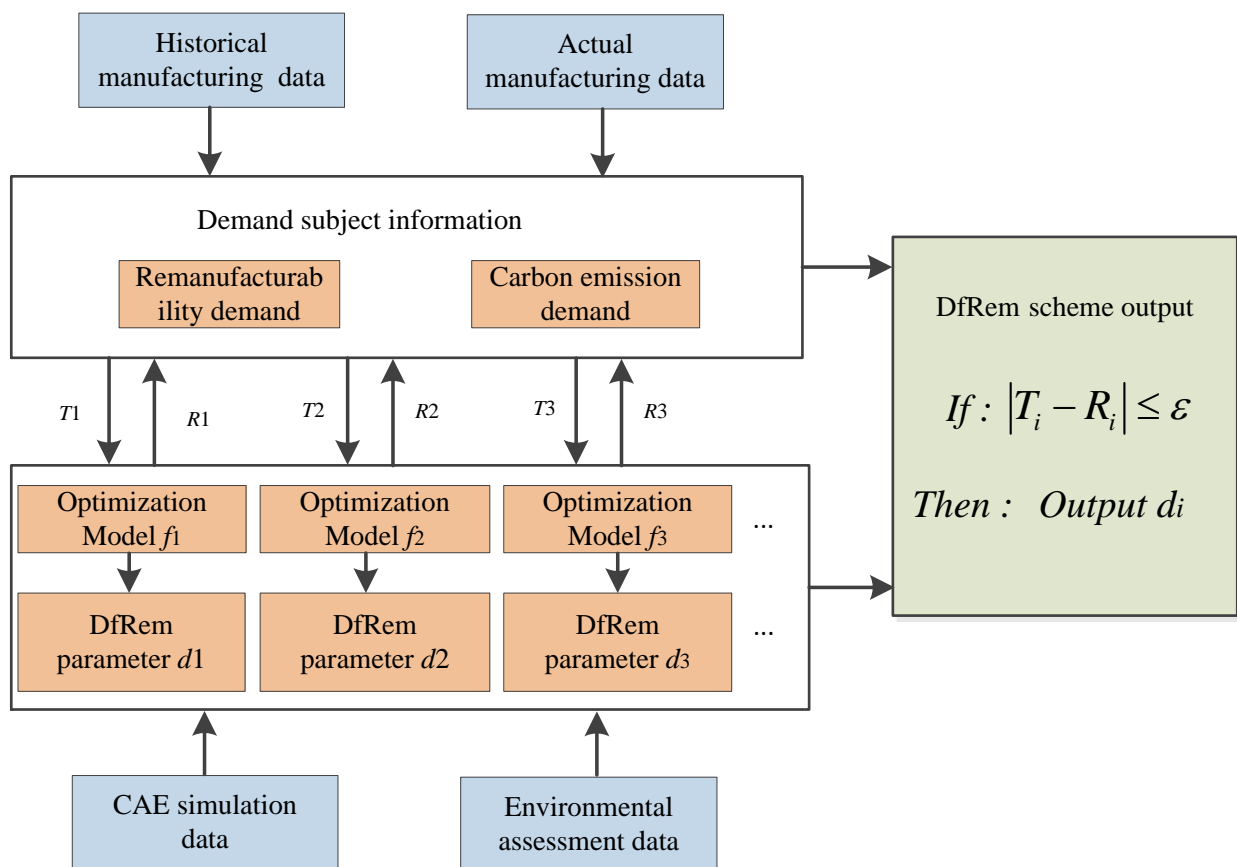


**Figure 3.** The optimization model framework of DfRem scheme.

#### 2.4. Optimization Model Solution

Multi-objective optimization model-solving algorithms have been developed very maturely. Commonly used examples include particle swarm algorithms, genetic algorithms, and ant colony algorithms, but these algorithms have insufficient computational accuracy and poor stability. In order to solve the limitations of previous algorithms, an adaptive teaching–learning-based optimization (ATLBO) algorithm is proposed, and the specific solving process is as follows (Figure 4).

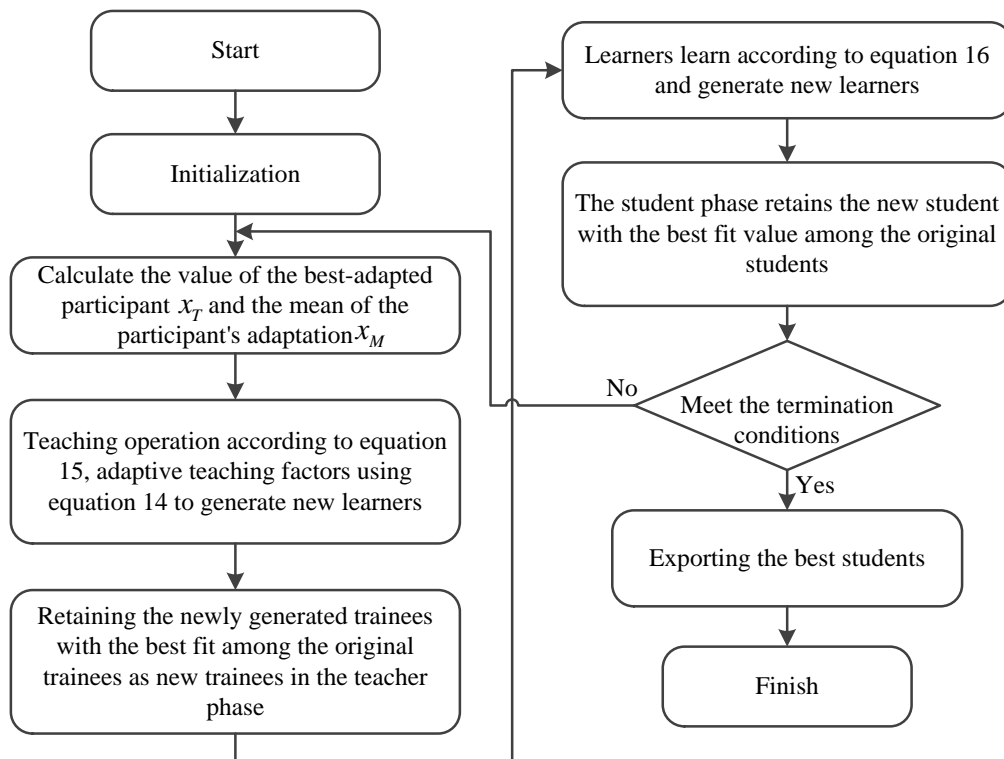


**Figure 4.** Adaptive teaching–learning-based optimization algorithm process.

#### 2.4.1. Teacher stage

In the teacher stage, learning is based on the differences between teachers and students, and first, the degree of difference in the mean between teachers and students is calculated as follows.

$$dif = T_c(t) \cdot (x_T - \theta \cdot x_M) \quad (12)$$

$$\theta = round(1 + rand(0,1)) \quad (13)$$

$$T_c(t) = \frac{1}{2} \cdot (T_{cmax} - T_{cmin}) \cdot \left( \frac{t_{max} - t_i}{t_{max}} \right)^2 + \frac{1}{2} \cdot (T_{cmax} - T_{cmin}) \cdot \left( \frac{t_{max} - t_i}{t_{max}} \right) + T_{cmin} \quad (14)$$

In Equation (12),  $x_M$  denotes the mean of the  $M$ -th learner,  $x_T$  denotes the mean of the teacher,  $T_c(t)$  denotes the adaptively adjustable learning factor,  $T_{cmax}$  denotes the maximum value of the learning factor,  $T_{cmin}$  denotes the minimum value of the learning factor,  $t_i$  denotes the number of iterations of the learning process, and  $t_{max}$  denotes the maximum number of cycles of the iterations.

In addition, students learn according to the differences with their teachers; the details are as follows:

$$x_{inew} = x_i + dif \quad (15)$$

where  $x_i$  denotes the value before the  $i$ -th participant, and  $x_{inew}$  denotes the value after the  $i$ -th participant's study.

#### 2.4.2. Student Stage

In the student phase, each participant randomly finds a learning target in the class for comparative analysis and adjusts the school factor according to the gap with the learning target, which is calculated as follows.

$$x_{inew} = \begin{cases} x_i + rand(0, 1) \cdot (x_j - x_i) & f(x_i) > f(x_j) \\ x_i + rand(0, 1) \cdot (x_j - x_i) & f(x_i) < f(x_j) \end{cases} \quad (16)$$

#### 2.4.3. Termination Guidelines

If the maximum number of iterations is reached, the calculation is terminated, and the optimization parameters are output; otherwise, the calculations in Steps A and B are repeated.

### 3. Case Study

To verify the feasibility of the proposed method, the DfRem of an injection mold is taken as an example. An injection mold is a key device for producing plastic products, which is shown in Figure 5. However, during the service process of the mold, it is found that the cavity surface is easily worn and corroded, which is not conducive to reprocessing the mold at the end of life. Moreover, the cooling area is not enough, and the poor cooling effect will affect the surface accuracy of plastic products, so designers need to optimize mold design parameters to solve the above problems. Meanwhile, in response to the ‘double carbon policy’, the manufacturing process scheme should satisfy the low carbon requirements.

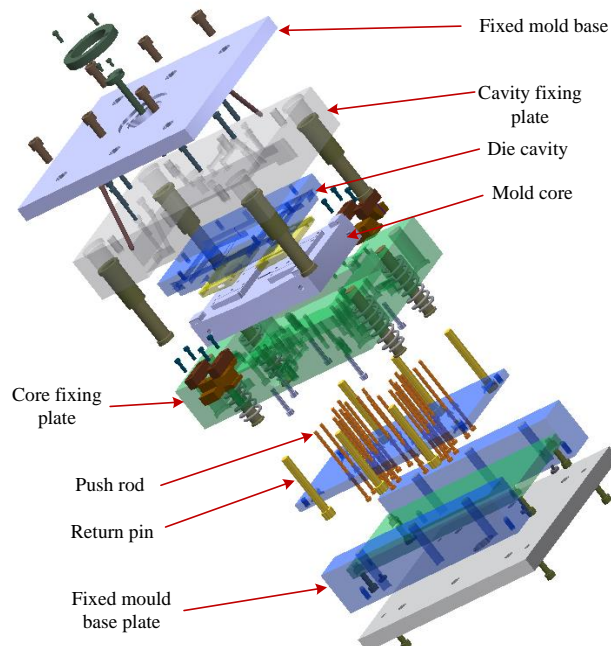


**Figure 5.** The structure of the mold.

First, heat treatment is used to improve the surface strength of the cavity; the empirical formula for carbon content and die surface tensile strength is shown as follows:

$$\sigma_b = 300(1 - C/0.83) + 1000(C/0.83) \quad (17)$$

where  $\sigma_b$  denotes the tensile strength of the mold, and  $C$  denotes the carbon content of the mold.

In addition, the cooling temperature is related to the cooling area, and the cooling area is related to the length and diameter of the cooling pipe; thus, the calculation formulae are as follows:

$$\Delta\theta = \frac{WQ}{Ah} \quad (18)$$

$$A = 3.14Ld \quad (19)$$

$$\Delta\theta = \frac{WQ}{3.14Ldh} \quad (20)$$

where  $\Delta\theta$  denotes the temperature difference between the outlet and inlet of the mold;  $W$  denotes the total mass of plastic melt injected into the mold cavity per unit time, in units of kg/h;  $Q$  is the heat released per unit mass of plastic part during solidification;  $L$  is the length of the cooling pipe;  $d$  denotes the diameter of the cooling pipe; and  $h$  denotes the heat transfer coefficient between the wall of the cooling pipe orifice and the cooling medium, in units of  $m^2 \cdot h^{-1} \cdot ^\circ C$ . The details are as follows (Table 1).

**Table 1.** Energy and material consumption.

DfRem Parameter	Energy and Material	Consumption	Carbon Emission
Cooling tube processing length (L)	Aluminum	0.3 kg	3.496 kg CO <sub>2</sub>
	Electricity	0.7398 kW · h	
Carbon content of parts (C)	Electricity	1.1313 kW · h	1.081 kg CO <sub>2</sub>
	Water	0.8 kg	
	Natural gas	0.0075 m <sup>3</sup>	

The sensitivity of DfRem parameters to carbon emissions can be calculated according to Equation (4), and the results are as follows.

From Table 2, it can be seen that the design parameter  $DP_1$  is positively correlated with carbon emissions, and  $DP_2$  is negatively correlated with carbon emissions; thus, the functional relationships between each design parameter and carbon emissions are as follows.

$$H_1 = 0.03802DP_1 - 7.91 \quad (21)$$

$$H_2 = -0.1302DP_2 + 1.1206 \quad (22)$$

$$H = 0.03802DP_1 - 0.1302DP_2 - 6.7894 \quad (23)$$

**Table 2.** Sensitivity analysis of DfRem parameters.

DfRem Parameter	Standard Design Parameters	Carbon Emission	Sensitivity S
Cooling tube length ( $DP_1$ )	300 mm	3.496 kg CO <sub>2</sub>	0.03802
Cavity carbon content ( $DP_2$ )	0.3%	1.081 kg CO <sub>2</sub>	-0.1302

According to Equations (17) and (20), as well as square original design information can be obtained as a function of the performance parameters and design parameters; the details are as follows:

$$f_1 = 300(1 - DP_2/0.83) + 1000(DP_2/0.83) \quad (24)$$

$$f_2 = \frac{WQ}{3.14 \cdot DP_1 \cdot d \cdot h} = \frac{3.811 \times 590}{3.14 \times 8 \times 1.4 \times DP_1} = \frac{2248.49}{35.168 \cdot DP_1} \quad (25)$$

Then, the multi-objective optimization model of the design solution regarding the performance parameters and carbon emission parameters is as follows.

$$\begin{cases} \min F_1 = \frac{1}{f_1} = \frac{1}{300(1- DP_2/0.83) + 1000(DP_2/0.83)} \\ \min F_2 = \frac{1}{f_2} = \frac{35.168 DP_1}{2248.49} \\ \min H = 0.03802 DP_1 - 0.1302 DP_2 - 6.7894 \end{cases} \quad (26)$$

s.t.

$$\begin{cases} 270mm \leq DP_1 \leq 1350mm \\ 0.28\% \leq DP_2 \leq 0.4\% \end{cases}$$

In the above equations, the length of the cooling tube  $DP_1$  should not be lower than the length of the concave die, the width of the cooling tube should not exceed the width of the concave die, and the spacing of the cooling tube is generally five times the diameter of the tube, so the above rules can be obtained as a constraint range. The range of carbon content  $DP_2$  is obtained by checking the material properties of P20 steel.

The adaptive teaching and learning algorithm was used to solve the multi-objective optimization model for the design solution, setting the number of students to 10, the number of students studying the course to 2 (the number of design variables), and the number of iterations to 50. In order to show the superiority of ATLBO, the conventional teaching and learning algorithm was run simultaneously, the results were compared, and the computational results are shown below.

From Figure 6, it can be seen that the ATLBO algorithm computes the multi-objective function iteratively up to Step 5, while the TLBOA computes iteratively up to Step 12 before convergence, indicating that the ATLBO algorithm computes faster.

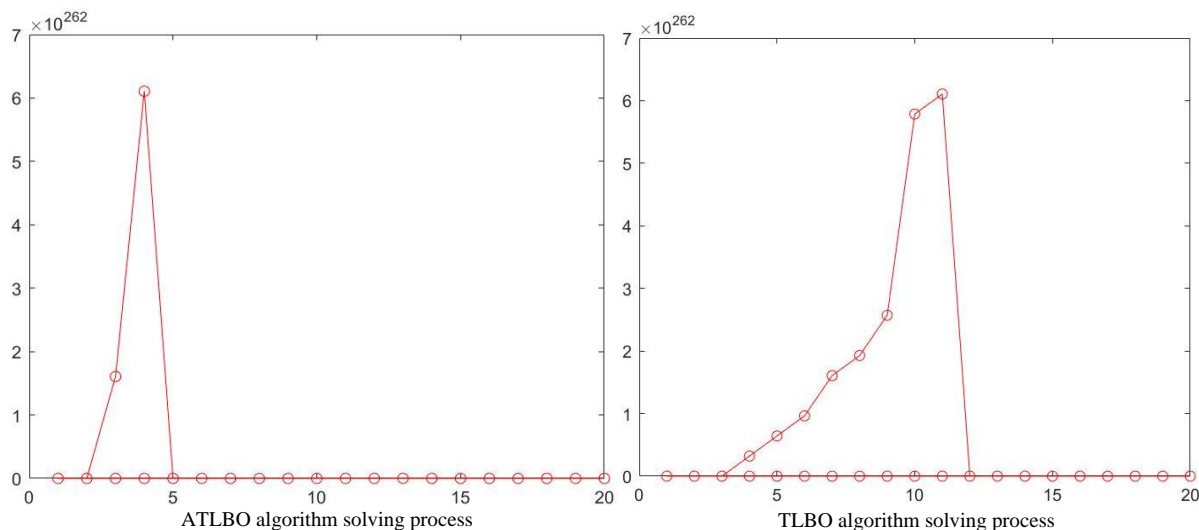


**Figure 6.** Comparison of ATLBO and TLBO algorithm solving process.

As can be seen in Figure 7, the results of the ATLBO and TLBO solutions are approximately the same, but ATLBO provides better convergence. To verify the reliability of the ATLBO algorithm, the computational quality data of the two algorithms are extracted for comparison, and the results are as follows.

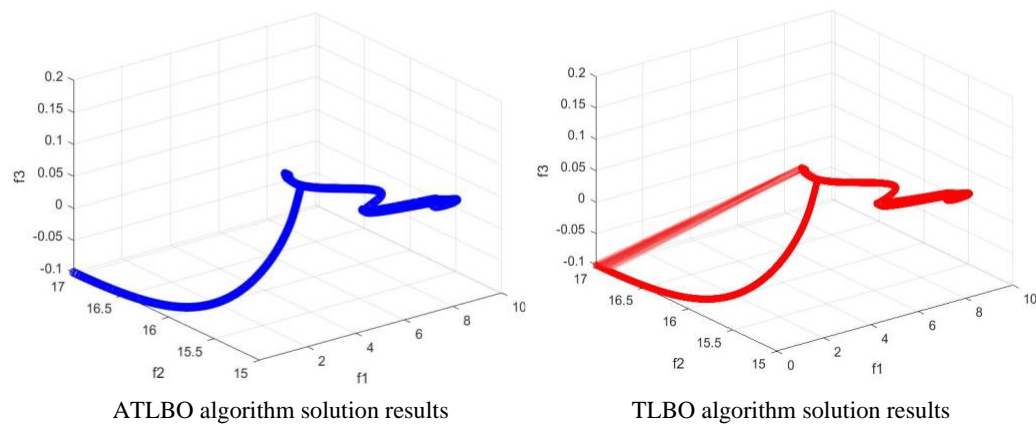


**Figure 7.** Comparison of ATLBO and TLBO algorithm solution results.

As can be seen in Figure 8, the quality values of the ATLBO solution process tend to a steady state, and the dip state tends to be smooth at the end of the iteration, while the quality values of TLBO are in a dip state and cannot be stabilized. This is because the adaptive teaching and learning algorithm continuously adjusts the learning strategy during the solution process, which can solve the objective function more stably and quickly; the solution results are shown below.

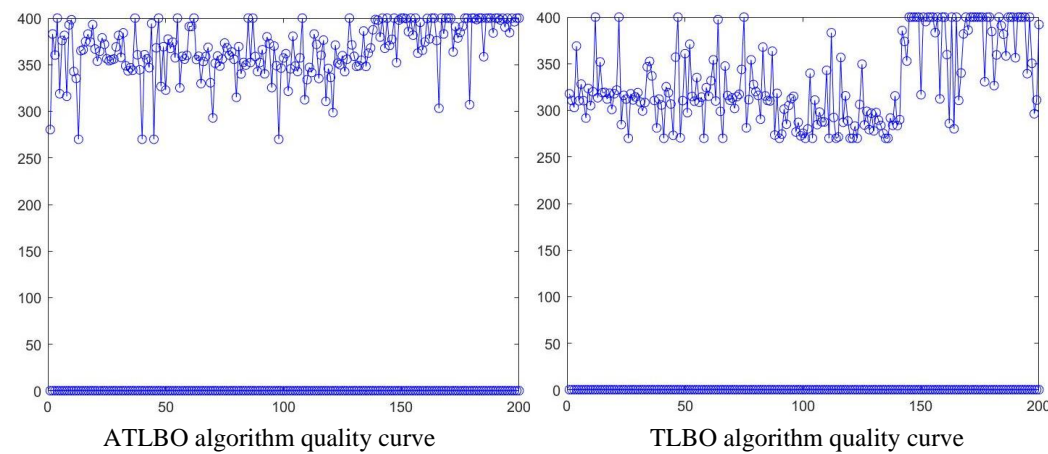


**Figure 8.** Comparison of solution quality between ATLBO and TLBO algorithms.

According to Table 3, both algorithms were able to solve for the design parameters that met the requirements; however, the ALBO algorithm was able to reduce the carbon emissions by 14.6%, reduce the internal temperature of the mold by 2 °C, and slightly increase the tensile strength than the design parameters solved by the TLBO algorithm. Overall, the ATLBO algorithm produced better and faster design solutions than TLBO.

**Table 3.** Comparison of optimization results for design parameters.

Algorithm	Design Parameter		Carbon Emission	Tensile Strength	Temperature Difference
	DP1	DP2			
ATLBO	298.2 mm	0.035%	4.5481 kg CO <sub>2</sub>	302.94 Mpa	1 °C
TLBO	314.67 mm	0.030%	5.2106 kg CO <sub>2</sub>	302.52 Mpa	3 °C

In order to verify the reliability of the optimization scheme, virtual simulation was used to verify the design scheme. Firstly, SolidWorks software 2020 was used to build

a 3D model of the injection mold, while the Sustainability module was applied to solve the carbon emission and energy consumption of the mold manufacturing process, and Moldflow software 2019 was used to simulate the performance of the mold, the specific results are as follows.

From the simulation analysis results in Figures 9–11, we can obtain the manufacturing costs of the mold, the cooling effects, and the carbon emissions of the manufacturing process. The mold manufacturing cost is USD 81.95, while the cost control requirement of the manufacturer is not more than USD 100 (excluding labor, equipment, and management costs). Therefore, the total remanufacturing cost is less than the manufacturer's expected maximum cost. Although the overall length of the cooling pipe is shorter due to the increase in the cooling pipe inlet and outlet, it can cool the molded part more directly and prevent uneven cooling, which affects the quality of the molded part, the carbon emission simulation analysis of the mold manufacturing process using the Sustainability module of SolidWorks shows that the carbon emission of the manufacturing process is 70 kg CO<sub>2</sub>, which is consistent with the manufacturer's historical carbon emission measurement. The results of the concave mold stress simulation in Figure 12 show a maximum yield stress of 282.7 Mpa and a maximum deflection of  $1.14615 \times 10^{-5}$  mm at this time. By comparing the optimized mold design with the design requirements, the error value between the two is within the allowable range, and the design can be output directly.



**Figure 9.** Mold manufacturing cost simulation analysis.

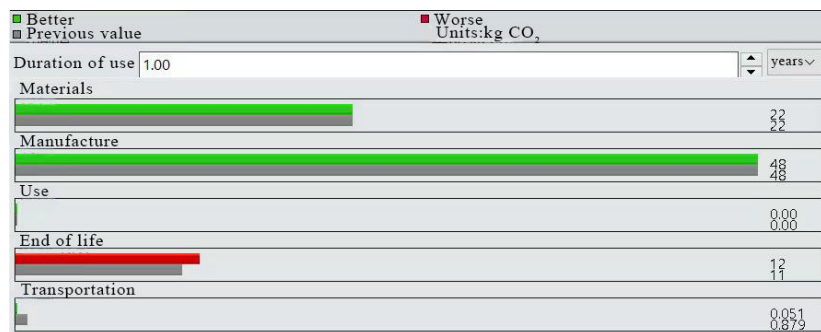


**Figure 10.** Carbon emissions from the mold manufacturing process.

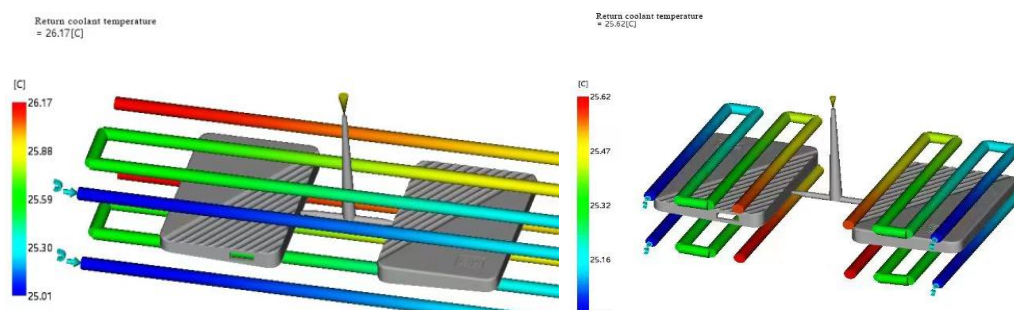


**Figure 11.** Comparison before and after improvement of the mold cooling pipes.

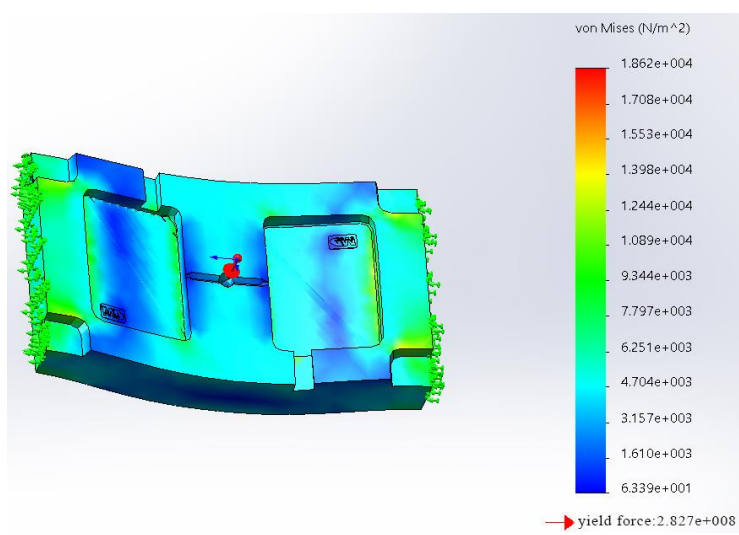


**Figure 12.** Stress distribution in the concave die.

From the results of the case study, it can be seen that the proposed design method can reduce carbon emissions and costs in the mold manufacturing process while improving the performance of the mold. This promotes the application of intelligent DfRem and provides a new theoretical model for DfRem methods.

#### 4. Conclusions and Future Work

Design for remanufacturing is an important process that affects not only the product remanufacturability but also the manufacturing carbon emission. To rapidly develop a rational design scheme for reducing manufacturing carbon emissions and improving product remanufacturability, this paper proposes an intelligent design method for remanufacturing that can obtain the design scheme for satisfying the design targets. The proposed methodology is able to balance the impact of design solutions on manufacturing carbon emissions and product remanufacturability, greatly reducing carbon emissions and increasing the utilization of used products, making green design more comprehensive. The following are some findings coming from this study:

- (1) An intelligent design framework for remanufacturing is constructed, which includes the construction of a mapping model between design parameters and carbon emissions and product remanufacturability. The design optimization model and solution method are also constructed, and the theoretical method for adaptive adjustment of design solutions is proposed.
- (2) Design matrix and sensitivity analysis were used to construct mathematical models of remanufacturability and carbon emissions in relation to design parameters.
- (3) The DfRem optimization model was constructed and intelligently solved with the ATLBO algorithm; the optimized design parameters can greatly reduce the manufacturing carbon emissions and improve mold cavity surface wear resistance and cooling effects.

For future work, there is a need to develop an intelligent method that can quickly simulate the optimized design scheme and verify its feasibility. Digital twin technology can truly portray the manufacturing and remanufacturing process of the products and make real-time corrections to design parameters based on manufacturing and remanufacturing process data, which helps designers optimize DfRem schemes more intuitively and quickly. Meanwhile, sensitivity analysis needs to be added to reflect the dynamic conditions affecting the results, and the method is only for the low-carbon design of products with remanufacturability demand, there is a need to establish a low-carbon design method for multiple types of demand; these will be studied in the future.

**Author Contributions:** Conceptualization, P.P.; methodology, C.K.; software, J.H. All authors have read and agreed to the published version of the manuscript.

**Funding:** This work was supported by the Wuhan Institute of Technology Research Foundation Project [K2023018] and the Sustainable Design and Product Ecological Innovation Team Project. These financial contributions are gratefully acknowledged.

**Data Availability Statement:** Data are contained within the article.

**Conflicts of Interest:** The authors declare no conflict of interest.

## References

1. Jiang, Z.; Jiang, Y.; Wang, Y.; Zhang, H.; Cao, H.; Tian, G. A hybrid approach of rough set and case-based reasoning to remanufacturing process planning. *J. Intell. Manuf.* **2019**, *30*, 19–32. [[CrossRef](#)]
2. Jiang, Z.; Ding, Z.; Liu, Y.; Wang, Y.; Hu, X.; Yang, Y. A data-driven based decomposition-integration method for remanufacturing cost prediction of end-of-life products. *Robot. Comput.-Integr. Manuf.* **2020**, *61*, 101838. [[CrossRef](#)]
3. Haziri, L.L.; Sundin, E. Supporting design for remanufacturing—A framework for implementing information feedback from remanufacturing to product design. *J. Remanuf.* **2020**, *10*, 57–76. [[CrossRef](#)]
4. Haziri, L.L.; Sundin, E.; Sakao, T. Feedback from Remanufacturing: Its Unexploited Potential to Improve Future Product Design. *Sustainability* **2019**, *11*, 4037. [[CrossRef](#)]
5. Gong, Q.S.; Zhang, H.; Jiang, Z.G.; Wang, H.; Wang, Y.; Hu, X.L. Nonempirical hybrid multi-attribute decision-making method for design for remanufacturing. *Adv. Manuf.* **2019**, *7*, 15. [[CrossRef](#)]
6. Ke, C.; Jiang, Z.; Zhang, H.; Wang, Y.; Zhu, S. An intelligent design for remanufacturing method based on vector space model and case-based reasoning. *J. Clean. Prod.* **2020**, *277*, 123269. [[CrossRef](#)]
7. Zhang, X.; Zhang, S.; Zhang, L.; Xue, J.; Sa, R.; Liu, H. Identification of product's design characteristics for remanufacturing using failure modes feedback and quality function deployment. *J. Clean. Prod.* **2019**, *239*, 117967. [[CrossRef](#)]
8. Yang, S.S.; Nasr, N.; Ong, S.K.; Nee, A.Y. Designing automotive products for remanufacturing from material selection perspective. *J. Clean. Prod.* **2017**, *153*, 570–579. [[CrossRef](#)]
9. Kishawy, H.A.; Hegab, H.; Saad, E. Design for sustainable manufacturing: Approach, implementation, and assessment. *Sustainability* **2018**, *10*, 3604. [[CrossRef](#)]
10. Soh, S.L.; Ong, S.K.; Nee, A.Y.C. Design for assembly and disassembly for remanufacturing. *Assem. Autom.* **2016**, *36*, 12–24. [[CrossRef](#)]
11. Shahbazi, S.; Johansen, K.; Sundin, E. Product Design for Automated Remanufacturing-A Case Study of Electric and Electronic Equipment in Sweden. *Sustainability* **2021**, *13*, 9039. [[CrossRef](#)]
12. Chakraborty, K.; Mondal, S.; Mukherjee, K. Analysis of product design characteristics for remanufacturing using Fuzzy AHP and Axiomatic Design. *J. Eng. Des.* **2017**, *28*, 338–368. [[CrossRef](#)]
13. Ai, X.; Jiang, Z.; Zhang, H.; Wang, Y. Low-carbon product conceptual design from the perspectives of technical system and human use. *J. Clean. Prod.* **2020**, *244*, 118819. [[CrossRef](#)]
14. Wang, Q.; Li, B.; Chen, B.; Wang, Z.; Liu, W.; Cheng, Y. Impact of product design on remanufacturing under environmental legislation. *Comput. Ind. Eng.* **2022**, *165*, 107889. [[CrossRef](#)]
15. Wang, Q.; Tang, D.; Li, S.; Yang, J.; Salido, M.A.; Giret, A.; Zhu, H. An Optimization Approach for the Coordinated Low-Carbon Design of Product Family and Remanufactured Products. *Sustainability* **2019**, *11*, 460. [[CrossRef](#)]
16. Zhang, L.; Jiang, R.; Jin, Z.F.; Huang, H.H.; Li, X.Y.; Zhong, Y.J. CAD-based identification of product low-carbon design optimization potential: A case study of low-carbon design for automotive in China. *Int. J. Adv. Manuf. Technol.* **2019**, *100*, 751–769. [[CrossRef](#)]
17. Peng, J.; Li, W.; Li, Y.; Xie, Y.; Xu, Z. Innovative product design method for low-carbon footprint based on multi-layer carbon footprint information. *J. Clean. Prod.* **2019**, *228*, 729–745. [[CrossRef](#)]
18. He, B.; Wang, J.; Deng, Z. Cost-constrained low-carbon product design. *Int. J. Adv. Manuf. Technol.* **2015**, *79*, 1821–1828. [[CrossRef](#)]
19. Li, Y.P.; Zhang, M.T.; Chen, D.P. Product obsolescence assessment based on the hybrid uncertain Information Axiom. *J. Eng. Des.* **2021**, *32*, 375–396. [[CrossRef](#)]
20. Cavique, L.; Cavique, M.; Mendes, A.; Cavique, M. Improving information system design: Using UML and axiomatic design. *Comput. Ind.* **2022**, *135*, 103569. [[CrossRef](#)]
21. Chen, J.; Tang, J.; Yang, D. Study on sensitivity analysis of tooth surface roughness parameters and contact stress. *J. Northwest. Polytech. Univ.* **2022**, *40*, 883–891. [[CrossRef](#)]
22. Zhang, X.; Liu, C.; Zhao, B. An optimization research on groove textures of a journal bearing using particle swarm optimization algorithm. *Mech. Ind.* **2021**, *22*, 1. [[CrossRef](#)]
23. Xue, D.; Imaniyar, D. An Integrated Framework for Optimal Design of Complex Mechanical Products. *J. Comput. Inf. Sci. Eng.* **2021**, *21*, 1–32. [[CrossRef](#)]

24. Tao, X.R.; Pan, Q.K.; Gao, L. An efficient self-adaptive artificial bee colony algorithm for the distributed resource-constrained hybrid flowshop problem. *Comput. Ind. Eng.* **2022**, *169*, 108200. [[CrossRef](#)]
25. Mi, X.; Liao, Z.; Li, S.; Gu, Q. Adaptive teaching-learning-based optimization with experience learning to identify photovoltaic cell parameters. *Energy Rep.* **2021**, *7*, 4114–4125. [[CrossRef](#)]

**Disclaimer/Publisher's Note:** The statements, opinions and data contained in all publications are solely those of the individual author(s) and contributor(s) and not of MDPI and/or the editor(s). MDPI and/or the editor(s) disclaim responsibility for any injury to people or property resulting from any ideas, methods, instructions or products referred to in the content.